Infrared Multispectral Monitoring of Cereal Crops

Massimo Rippa*[a], Rossella Curcio[a], Ida Di Mola[b], Lucia Ottaiano[b], Eugenio Cozzolino[c], Mauro Mori[b], Pasquale Mormile[a]

[a]Institute of Applied Sciences and Intelligent Systems "E. Caianiello" of CNR, via Campi Flegrei 34, 80072 Pozzuoli (Na), Italy
[b]Department of Agricultural Sciences, University of Naples Federico II, Portici, 80055, Italy
[c]Council for Agricultural Research and Economics (CREA)—Research Center for Cereal and Industrial Crops, Caserta, 81100, Italy

*m.rippa@isasi.cnr.it, phone +390818675334, https://www.isasi.cnr.it/en/image-sensing-for-agricultural-cultural-heritage-and-ndt-applications/

ABSTRACT

Plants are subjected to a wide range of stresses which reduces the productivity of agricultural crops. In the case of cereal cultivations, climate change impacts on their production mainly through abiotic and biotic stress due for example to heat and water stress but also to pathogens such as bacteria, fungi, nematodes and others. The area under cereal cultivation is increasing worldwide, but, due to these problems, the current rates of yield growth and overall production are not enough to satisfy future demand. For this motivation, there is the needs to monitor and to control the cultivations, also developing new technological solutions useful to better optimize the management strategies, increasing both the quality of products and the quantity of the annual cereal harvest. Infrared imaging is a well-known non-invasive and non-contact technique that represents an outstanding approach of analysis applied in many fields: engineering, medicine, veterinary, cultural heritage and others. In recent years it has been gaining great interest in agriculture as it is well suited to the emerging needs of the precision agriculture management strategies. In this work, we performed an in-field multispectral infrared monitoring of different cereal crops (durum wheat and common wheat) through the use of both LWIR and MWIR cameras. The monitoring carried out made it possible to identify, among the crops analyzed, those subject to higher stress levels and their response to the different spectral ranges used. The results obtained open to the possibility of identifying new figures of merit useful for an effective monitoring of cereal crops and measurable through remote instrumentation.

Keywords: Thermography, Digital Agriculture, Precision Agriculture, Cereals, Infrared Imaging, Plant Stress

1. INTRODUCTION

Cereals are used as raw material for many foods around the world and in particular in the Mediterranean basin.[1,2] Wheat constitutes one of the most cultivated cereals thank to its versatility for the preparation of various foods and to its nutritional value in the human diet.[3,4] They are often subjected to a wide range of stresses which reduces their productivity. Climate change as well as others abiotic and biotic stress due for example to heat and water stress but also to pathogens such as bacteria, fungi, nematodes might be responsible for larger or smaller changes in their crop yields.[5] Moreover, adaptation to specific climatic and territorial conditions of the Mediterranean area can play an important role in their growth. Due to these problems, the current rates of yield growth and overall production are not enough to satisfy future demand. For this motivation, there is the needs to monitor and to control the wheat crops, also developing new technological methods to optimize the management strategies, increasing both the quality of products and the quantity of the annual harvest. Wheat monitoring based on imaging techniques is an interesting approach to quantify both the state of health and the performance of crops under different environmental conditions. Among these techniques, infrared imaging is a well-known non-invasive and non-contact method that represents an outstanding approach of analysis applied in many fields, from agriculture to non-destructive testing.[6-16] As reported in literature, it is essential to determine the temperature demands in each phenological stage in order to account for the variations in wheat yield due to climatic conditions.[17,18] In recent years, this technique has been used to evaluate physical and physiological characteristics of plants among which: transpiration rates, heat capacity of the leaves, local water content, water flow velocity, response to UV interaction.[19-23] Moreover, it proved to be a valuable tool for the diagnosis and detection of plant to different kind of biotic and abiotic stress, adapting well to the emerging needs of precision agriculture management strategies.[24,25] Infrared imaging was extensively used for proximal (in field, in growth chambers and in greenhouses) or remote sensing (drones and UAVs systems) of plant stress. In this work, realized in the frame of the Italian regional project "Valorizzazione della BIOdiversità cerealicola in regime BIOlogico - BIOeBIO" (PSR Campania 2014-2020), it was performed a multispectral infrared monitoring of different varieties of wheat crops (durum and common) realized on both proximal and remote scale. The performance of two cameras with sensors in the spectral range respectively Long Wave Infrared (LWIR) and Mid Wave Infrared (MWIR) were tested and compared, in the specific environmental condition of the experimental field to monitor the state of different varieties of wheat. Furthermore, the analysis performed made it possible to compare and to identify, among the monitored varieties, those ones subject to higher stress levels during the different phenological stages of growth and the respective percentages of soil coverage introducing two indices for their estimation. The results achieved give interesting information concerning both the development of novel infrared monitoring systems and the level of adaptation of the wheat varieties monitored to the specific climatic conditions of growth to which they were subjected, typical of the Mediterranean area.

2. MATERIALS AND METHODS

Infrared measurements

Infrared measurements were performed using both a MWIR camera FLIR X6580 sc with a cooled indium antimonide (InSb) detector (FPA 640x512 pixels and NETD ~20 mK at 25 °C) mounting a 50 mm focal lens with spectral band 3.5-5 µm and IFOV 0.3 mrad and a LWIR AVIO TVS500 with an uncooled microbolometric detector (spectral range 8–14 µm, FPA 320 × 240 pixels and NETD ~ 60 mK at 25 °C) mounting a 22 mm focal lens with IFOV 1.68 mrad. The commercial software, ResearchIR (FLIR Systems) and IRT Analyzer (GRAYESS inc.), with which the cameras are supplied, are used for monitoring the temperature in real-time and for basic operations. Figure 1 shows pictures of the two cameras (MWIR 1a and LWIR 1b) and a table (1c) reporting their main technical characteristics.

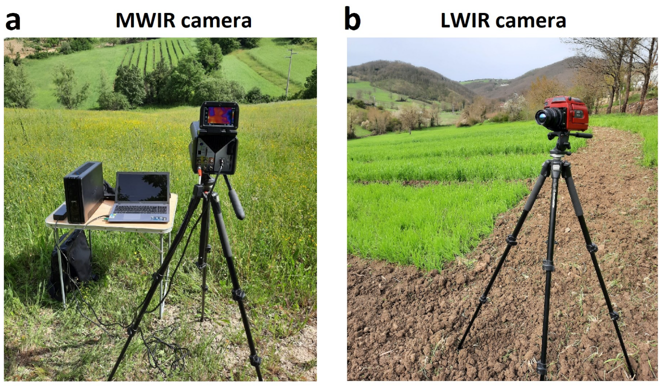

c

Device	IR Range	Detector	FPA Resolution	NEDT (25°C)	iFOV (x,y) cm/pixel
FLIR X6580 c	MWIR (3.5-5 µm)	InSb (cooled)	640x512	20 mK	0.3 mrad
AVIO TVS500	LWIR (8-14 µm)	VO_x (uncooled)	320x240	50 mK	1.68 mrad

Figure 1. Pictures of the two cameras used for the infrared monitoring, a) MWIR and b) LWIR and c) table reporting their main technical characteristics.

Experimental design and plant materials

Field measurements were carried out during the growing seasons 2021-2022, on two private farms located in the Alto Tammaro area (Benevento area, Campania Region – Italy), specifically in Colle Sannita (Latitude: 41° 22’ 48.5’’ N, Longitude: 14° 52’ 09.5’’ E, Altitude: 695 m) and in Castelpagano (Latitude: 41° 25’ 50.7’’ N, Longitude: 14° 48’ 15.1’’ E, Altitude: 805 m). In the first farm, five different varieties of durum wheat were compared: Pigreco, Svevo, Saragolla, Senatore Cappelli, and Marzellina, of which the last three are traditional varieties; in the second one, five varieties of common wheat were tested: Alteo, Taxum, Risciola, Romanella, and Gentil Rosso, and also in this case, the last three are traditional varieties. The sowings were made on December 21, 2021, with a density of 500 seeds per square meter.
Each experimental plot was 2.5 x 20 m and it was replicated three times. No fertilization nor interventions for weeds and pathogens control were made since both farms follow organic cultivation. Infrared monitoring was performed at four different phenological phases of the crops: steam elongation (April 21, 2022), heading begins (May 26, 2022), milky-waxy ripening (June 13, 2022) and full ripening (June 30, 2022). The harvests were made on July 11, 2022, in both farms.

3. RESULTS AND DISCUSSION

Comparison of MWIR and LWIR spectral ranges for wheat monitoring

Designing a high-performance monitoring system that can also operate remotely, based on infrared technologies, requires the optimization of various physical-optical parameters, among which the choice of the sensor and therefore of the spectral range to be used is a crucial point.
MWIR and LWIR sensors are developed using respectively photon and thermal detectors. Photon detectors boast many technical advantages respect the thermal counterpart, including fast response and a lower signal to noise ratio. On the other side, thermal detectors are lighter and less expensive substantially due to the absence of a cooling system necessary instead for photonic sensors which are based on the use of semiconductors. However, the optimal choice is closely linked both to the type of samples to be investigated and to the average atmospheric conditions present during the experimental measurements. In order to provide more information on this aspect, in this work infrared measurements of five plots of durum wheat, taken at heading begins growing phase (May 26, 2022), were realized using two thermal cameras respectively in the LWIR and MWIR spectral ranges in both proximal and remote scale.
In figure 2 are reported the main information achieved with both camera on five type of durum wheat realized in remote scale, from a hill at about 350 m from the experimental field.

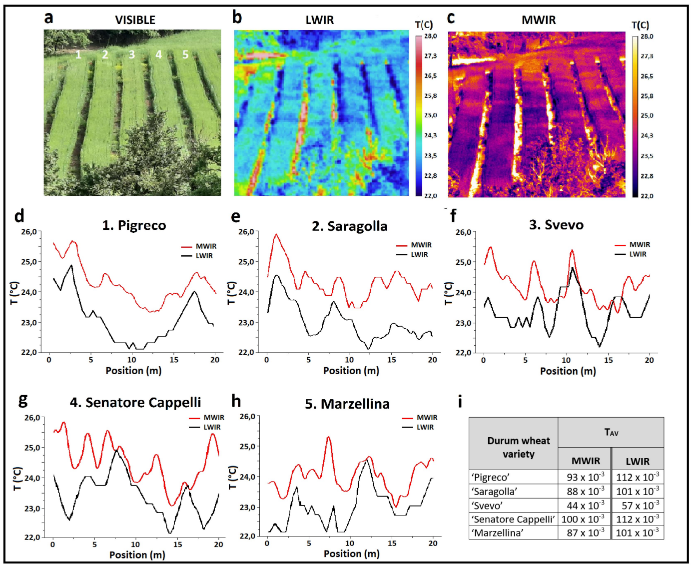

Figure 2. Comparison of the infrared monitoring realized on remote scale using two spectral ranges: a) visible image of the plots of the five durum wheat varieties, b) LWIR and c) MWIR image images of the experimental field, d)-h) comparison of the temperature profiles measured with the two cameras on the five durum wheat monitored, i) table reporting the T_{AV} values estimated for the five crops.

In particular, figures 2a-c show a comparison between a visible, a LWIR and a MWIR image of the experimental field while figures 2d-h report the temperature profiles measured with the two cameras (red lines MWIR, black lines LWIR) taken from top to bottom of the crop rows.
As visible from the graphs, in all cases the profiles achieved in the MWIR range shows higher temperatures than those measured in the LWIR range. This achievement can be explained considering the atmospheric condition during which the measurements were realized, characterized by a mean environmental temperature of 27°C and a humidity in the range 75 -78%, typical values in the months of May-June for the geographical area in which the experimental field is located. In fact, as well known, sensors based on MWIR range has higher transmittivity under high humidity and clear weather performance, whereas sensor based on LWIR range shows performs better in fog, dust conditions having a higher tolerance to atmospheric turbulence.[26] From the data acquired we calculate the average canopy temperature index $T_{AV} = (T_{MAX}-T_{MIN})/T_{MAX}$ where T_{MAX} and T_{MIN} are the maximum and the minimum average temperature measured on the crop rows respectively.[27,28] The values achieved with the two spectral ranges for the five durum wheat varieties monitored are reported and compared in the table reported in figure 2i. The results obtained indicate how, in the specific atmospheric condition of measurement, the data acquired in the LWIR range can induce an overestimation of this parameter thus making the assessments carried out with this type of sensor remotely (also for example through the use of drones and UAV systems) less reliable than those obtained in the MWIR range.
This difference in performance and reliability of the results is cleared in the case of evaluations carried out on a proximal scale. In figure 3, as an example, are reported experimental measurements realized on one durum wheat cultivation (‘Svevo’ variety) takes in proximal scale.

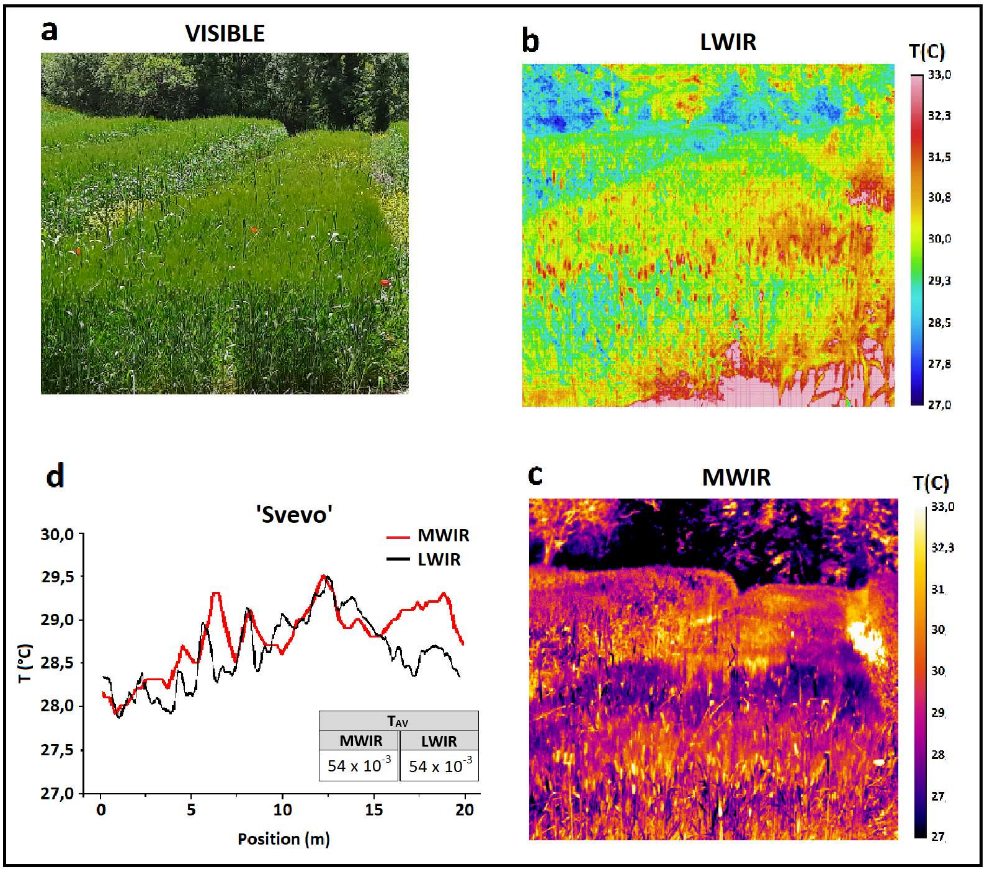

Figure 3. Comparison of the infrared monitoring realized on proximal scale using two spectral ranges: a) visible image of the plots of ‘Svevo’ variety, b) LWIR and c) MWIR image images of the experimental field, d) comparison of the temperature profiles measured with the two cameras on the soft wheat variety considered and table reporting the T_{AV} values estimated for the crop.

As in the case of remote analysis, figure 3a shows a visible image of the wheat, 3b and 3c a comparison between its LWIR and MWIR images respectively, while in figure 3d the temperature profiles measured with the two cameras.
As can be seen from the graph in 3d, even if the measured temperatures are slightly different, the T_{AV} index calculated and shown in the table, is practically the same. This last result highlights how the effects due to high humidity for measurements carried out on a proximal scale are negligible, and, therefore, also due to its lower commercial cost, the LWIR technology can be preferred to MWIR-based cameras in this type of experimentation.

Evaluation of the soil coverage of durum wheat varieties

From the infrared images acquired, the percentage of soil coverage by the various wheat crops monitored was evaluated. The analysis was performed in the steam elongation (April 21, 2022) phenological state of the crops. To achieve this parameter from each thermographic image acquired, the number of pixels associated with the vegetation (N_V) and those associated with the soil (N_S) were evaluated. In Figure 4, as an example, are shown a visible image of a cultivation clod (4a), the corresponding thermographic image (4b), and two of its representations in which only the pixels associated with the vegetation (4c) or with the soil (4d) are reported.

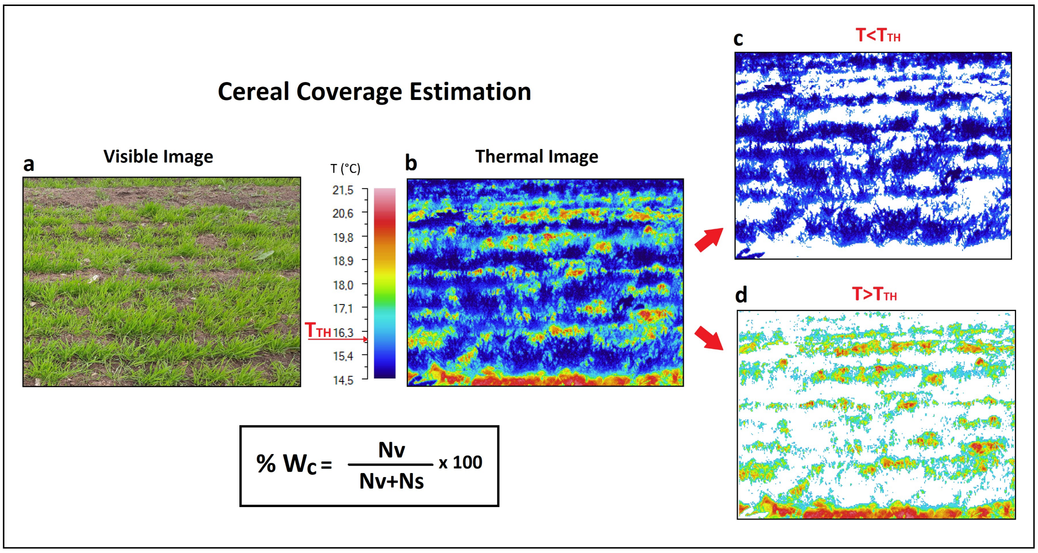

Figure 4. Analyses for cereal coverage estimation: a) visible image of a cultivation clod the corresponding thermographic image (4b), and two of its representations in which only the pixels associated with the vegetation (4c) or with the soil (4d) are reported.

The separation of the two classes of pixels was carried out considering the temperature diagram associated with the image where it is possible to identify a threshold value T_{TH} that allows to discriminate the temperature distribution of the vegetation and that of the soil (T_{TH} =16.1 °C in figure 4b). The pixels N_V that refer with vegetation are those with a temperature $T_V < T_{TH}$ while those that refer with the soil N_S with a temperature $T_S > T_{TH}$. The percentage of wheat coverage (% W_C) can therefore be calculated with the following relationship: $\%W_C = [N_V/(N_V+N_S)]x100$.
It must be said that this type of evaluation based on the choice of a T_{TH} is subject to an intrinsic error due to the presence of pixels in the diagram related with the vegetation having $T_V > T_{TH}$ and pixels related with the soil having $T_S < T_{TH}$. However, in the reasonable hypothesis that the number of such pixels is approximately equal and negligible respect both N_V and N_S, the proposed method allows an estimation of the percentage of soil coverage of wheat crops and a comparison of the different types of cereals rows considered. In table 1 the comparison of the $\%W_C$ values estimated for respectively five durum wheat varieties and five common wheat varieties monitored is reported.

Durum wheat variety	%Wc	Common wheat variety	%Wc
'Pigreco'	83	'Alteo'	85
'Saragolla'	91	'Risciola'	86
'Svevo'	92	'Romanella'	88
'Senatore Cappelli'	93	'Taxum'	83
'Marzellina'	89	'Gentil Rosso'	93

Table 1. Table reporting the $\%W_C$ values estimated for both durum and common wheat varieties monitored.

The values reported for each species of cereals represent the average calculated from five infrared images acquired randomly along the crops. $\%W_C$ estimated are in the range 83% - 93% for both wheat species with the highest values (93%) found in the case of the 'Senatore Cappelli' variety for durum wheat and 'Gentil Rosso' variety for common wheat.

Common wheat stress level monitoring: NRST index

Different varieties of common wheat were monitored throw the use of the infrared imaging in LWIR range, taking measurements in proximity scale, in order to evaluate their level of adaptability to the environmental conditions to which they are subjected during their growth period. Analysis were performed at four different phenological phases of the crops: steam elongation (April 21, 2022), heading begins (May 26, 2022), milky-waxy ripening (June 13, 2022) and full ripening (June 30, 2022), acquiring 20 thermal images for each variety along all the rows, randomly. As an example, in figure 5a, both a visible and a thermal image acquired in the four phases of growth are shown for one of the investigated variety.

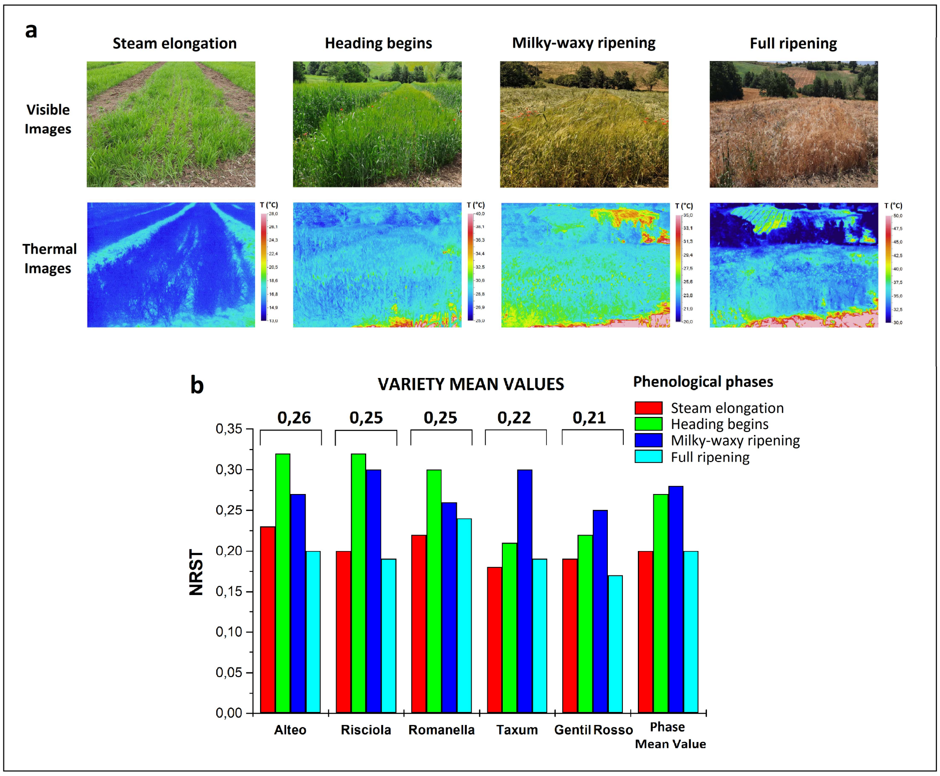

Figure 5. Analyses for the estimation of the stress level of cereals: a) visible and corresponding thermal images acquired in four phases of growth for one of the investigated variety, b) graph of the *NRST* index measured for each variety of common wheat monitored in the four phenological phases taken into account.

In the thermal images acquired, the pixels referring to vegetation and soil were separated as described in the previous section, and the mean values of the temperature of the wheat variety (T_{MW}) and of the soil (T_{MS}) were calculated in each growth phase analyzed. With these two values a new index, the Normalized Relative Soil Temperature (*NRST*) achieved with the following relation $NRST= (T_{MS} – T_{MW}) / T_{MS}$, was calculated. In table 2 and figure 5b, the *NRST* index obtained for each variety of common wheat in the four monitored phenological phases are showed and graphicated, respectively.

NRST Index					
Variety	Phenological phases				Variety mean value
	Steam elongation	Heading begins	Milki-waxy ripening	Full ripening	
'Alteo'	0.23	0.32	0.27	0.20	0.26
'Risciola'	0.20	0.32	0.30	0.19	0.25
'Romanella'	0.22	0.30	0.26	0.24	0.25
'Taxum'	0.18	0.21	0.30	0.19	0.22
'Gentil Rosso'	0.19	0.22	0.25	0.17	0.21
Phase Mean Value	0.20	0.27	0.28	0.20	

Table 2. Table reporting the *NRST* index obtained for each variety of common wheat at the four monitored phenological phases.

In all the measurements carried out we found $T_{MS} > T_{MW}$, therefore, from the *NRST* relation given above, lower *NRST* values corresponding with lower difference $T_{MS} – T_{MW}$ and vice versa. In general, this difference is smaller the higher the value of T_{MW}. In the hypothesis that this difference can be related to the stress level of the crop, lower values of *NRST* indicate a tendency of the vegetation to higher stress level while higher values of the same index a tendency to lower stress level and therefore greater adaptability of the variety. Considering the mean value of the *NRST* reported in the last column of table 2, 'Alteo' represents the variety that has shown higher adaptability to the environmental conditions of growth while 'Gentil Rosso' showed a higher mean stress level during the four growth stages monitored. Moreover, considering the phase mean values reported in the last row of the same table, both steam elongation and full ripening represent the phenological growth phases where all the varieties show higher mean stress level, and hence, based on our results, they represent the states that need more control and monitoring by the farmer.
Unlike other indices present in the literature normalized with respect to the air temperature T_{air} [29-31], the choice in the new index introduced here to consider the soil temperature as a reference is based on two main considerations: 1) the T_{MS} better describes the local environmental conditions to which a specific wheat row is subjected respect to T_{air}, as it is affected with higher sensitivity from any differences in both irradiation (presence of shaded areas) or soil moisture, 2) unlike the measurement of T_{air} that requires an additional instrument, T_{MS} can be extrapolated directly from the acquired thermal frames, thus facilitating the design of automatic and remote analysis systems.

4. CONCLUSIONS

In this work, we made an in-field infrared monitoring of different cereal varieties belonging to the durum wheat and common wheat species. A comparison between the information achieved on two spectral ranges LWIR and MWIR was carried out highlighting the advantages and criticalities of their use in both proximal and remote scales. Two indices for the estimation of soil coverage ($\%W_C$) and stress level (*NRST*) for wheat crops were introduced, calculated, and discussed. The results obtained provide useful information to identify new figures of merit and to design new infrared automatic detection systems that also meet the demands of precision agriculture strategies.

ACKNOWLEDGEMENTS

This activity is funded by the Italian regional project "Valorizzazione della BIOdiversità cerealicola in regimeBIOlogico - BIOeBIO" PSR Campania 2014-2020, GAL Alto Tammaro – GAL Titerno, Misura 16, Sottomisura 16.1.1.2, CUP - G22C21000320007.

REFERENCES

[1] Alfonzo, A., Sicard, D., Di Miceli, G., Guezenec, S. and Settanni, L., "Ecology of yeasts associated with kernels of several durum wheat genotypes and their role in co-culture with Saccharomyces cerevisiae during dough leavening." Food Microbiology 94:103666 (2020).

[2] Peña-Bautista, R.J., Hernandez-Espinosa, N., Jones, J.M., Guzmán, C. and Braun, H.J.,"CIMMYT series on carbohydrates, wheat, grains, and health: Wheat-based foods: Their global and regional importance in the food supply, nutrition, and health." Cereal Foods World 62:231-249 (2017).

[3] Braun, H.J., Atlin, G. and Payne, T.,"Multi-location testing as a tool to identify plant response to global climate change." In: Reynolds CRP (Ed). Climate Change and Crop Production. CABI, London, UK pp 115 (2010).

[4] Pomeranz, Y., "Bread around the world." In: Pomeranz Y (Ed). Modern Cereal Science and Technology. VCH Publishers, Inc., New York, USA pp 258 (1987).

[5] Carvajal-Yepes, M., Cardwell, K., Nelson, A., Garrett, K.A., Giovani, B., Saunders, D.G.O., Kamoun, S., Legg, J.P., Verdier, V., Lessel, J., et al., "A global surveillance system for crop diseases." Science, 364, 1237–1239 (2019).

[6] Ishimwe, R., Abutaleb, K. and Ahmed, F., "Applications of thermal imaging in agriculture - A review." Advanced Remote Sensing, 3, 128–140 (2014).

[7] Pineda, M., Barón, M. and Pérez-Bueno, M. L., "Thermal imaging for plant stress detection and phenotyping," Remote Sensing, 13(1), 68 (2021).

[8] Capraro, A. C. W., Steppe, K., Van Asten, P. J. A., Laderach, P., Jassogne, L. T. P. and Grab, S. W., "Application of thermography for monitoring stomatal conductance of Coffea Arabica under different shading systems," Science of the Total Environment, 609, 755–763 (2017).

[9] Vadivambal, R. and Jayas, D. S., "Applications of thermal imaging in agriculture and food industry—A review," Food and Bioprocess Technology, 4, 186–199 (2011).

[10] Guilioni, L., Jones, H. G., Leinonen, I. and Lhomme, J. P., "On the relationships between stomatal resistance and leaf temperatures in thermography," Agricultural and Forest Meteorology, 148, 1908–1912 (2008).

[11] Rippa, M., Battaglia, V., Cermola, M., Sicignano, M., Lahoz, E. and Mormile, P., "Monitoring of the copper persistence on plant leaves using pulsed thermography," Environ Monit Assess, 194:160 (2022).

[12] Oerke, E. C., Fröhling, P. and Steiner, U., "Thermographic assessment of scab disease on apple leaves," Precision Agriculture, 12, 699–715 (2011).

[13] Aryalekshmi, B. N., Biradar, R. C. and Mohammed Ahamed, J., "Thermal Imaging Techniques in Agricultural Applications" International Journal of Innovative Technology and Exploring Engineering 8(12), 2162-2168 (2019).

[14] Cohen, Y., Alchanatis, V., Sela, E., Saranga, Y., Cohen, S., Meron, S., Bosak, A., Tsipris, J., Ostrovsky, V., Orolov, V., Levi, A. and Brikman, R., "Crop water status estimation using thermography: Multi-year model development using ground-based thermal images" Precision Agriculture, 16, 311–329 (2015).

[15] Boccardi, S., Carlomagno, G.M., Meola, C., Russo, P. and Simeoli, G., "The contribution of infrared thermography in the characterization of jute based composites." Composite Structures 190, 119-126 (2018).

[16] Meola, C., Boccardi, S., Carlomagno, G.M., Boffa, N.D., Ricci, F., Simeoli, G. and Russo, P., "Impact damaging of composites through online monitoring and non-destructive evaluation with infrared thermography." NDT & E International 85, 34-42 (2017).

[17] Ayed, S., Othmani, A., Chaieb, N., Rezgui, M., Ben Younes, M., "Relation between agro-meteorological indices, heading date and biological/grain yield of durum wheat genotypes." Journal of Research in Agriculture and Animal Science 3(10):1-6 (2016).

[18] Tack, J., Barkley, A., Nalley, L.L., "Effect of warming temperatures on US wheat yields. Proceedings of the National Academy of Sciences. 112(22):6931-6936 (2015).

[19] Garbea, C. S., Schurrb, U. and Jähnea, B., "Thermographic measurements on plant leaves," Proceed. Thermosense XXIV, 4710, 1–9 (2002).

[20] Bonanomi, G., Battista Chirico, G., Palladino, M., Gaglione, S. A., Crispo, D. G., Lazzaro, U., Sica, B., Cesarano, G., Tushar, F. I., Sarker, C., Rippa, M. and Scala, F., "Combined application of photo-selective mulching films and beneficial microbes affects crop yield and irrigation water productivity in intensive farming systems" Agricultural Water Management, 184, 104–113 (2017).

[21] Blonquist, J. M., Jr., Norman, J. M. and Bugbee, B., “Automated measurement of canopy stomatal conductance based on infrared temperature,” Agricultural and Forest Meteorology, 149(11), 1931–1945 (2009).
[22] Bajons, P., & Klinger and G., Schlosser, V., “Determination of stomatal conductance by means of infrared thermography,” Infrared Physics & Technology, 46(5), 429–439 (2005).
[23] Rippa, M., Ambrosone, A., Leone, A. and Mormile, P., “Active thermography for real time monitoring of UV-B plant interactions,” Journal of Photochemistry and Photobiology b: Biology, 208, 111900 (2020).
[24] Zhou, Z., Majeed, Y., Diverres Naranjo, G. and Gambacorta, E.M.T., “Assessment for crop water stress with infrared thermal imagery in precision agriculture: A review and future prospects for deep learning applications.” Computers and Electronics in Agriculture 182, 106019 (2021).
[25] Galieni, A., D’Ascenzo, N., Stagnari, F., Pagnani, G., Xie, Q. and Pisante, M., “Past and Future of Plant Stress Detection: An Overview From Remote Sensing to Positron Emission Tomography.” Front. Plant Sci. 11:609155 (2021).
[26] Dakin, J. and Brown, R., “Handbook of optoelectronics (two-volume set)”. Taylor Francis (2010).
[27] Heermann, D., Duke, H., “Electrical load and water management.” Proc. Annu. Tech. Conf. 1978, 60–67 (1978).
[28] Jones, H.G., Stoll, M., Santos, T., de Sousa, C., Chaves, M.M., Grant, O.M., “Use of infrared thermography for monitoring stomatal closure in the field: Application to grapevine.” J. Exp. Bot., 53, 2249–2260 (2002).
[29] Idso, S.B., Jackson, R.D. and Reginato, R.J., “Remote-sensing of crop yields.” Science, 196, 19–25 (1977).
[30] Idso, S.B., Reginato, R.J., Jackson, R.D. and Pinter, P.J., “Foliage and air temperatures: Evidence for a dynamic “equivalence point”.” Agric. Meteorol, 24, 223–226 (1981).
[31] Jackson, R.D., Idso, S.B., Reginato, R.J. and Pinter, P.J., “Canopy temperature as a crop water stress indicator.” Water Resour. Res., 17, 1133–1138 (1981).